Supplemental Information file

Post-translational acylation controls the folding and functions of the CyaA RTX toxin

Darragh P. O'Brien[1]#, Sara E. Cannella[1]#, Alexis Voegele[1], Dorothée Raoux-Barbot[1], Marilyne Davi[1], Thibaut Douché[2], Mariette Matondo[2], Sébastien Brier[1]*, Daniel Ladant[1]* and Alexandre Chenal[1]*

Addresses

[1] Institut Pasteur, Chemistry and Structural Biology Department, UMR CNRS 3528, 75724 PARIS cedex 15, France

[2] Institut Pasteur, Proteomics Platform, Mass Spectrometry for Biology Unit, USR CNRS 2000, 75724 PARIS cedex 15, France

# these authors contributed equally to this work

* to whom correspondence and material requests should be addressed:
sebastien.brier@pasteur.fr; daniel.ladant@pasteur.fr; alexandre.chenal@pasteur.fr

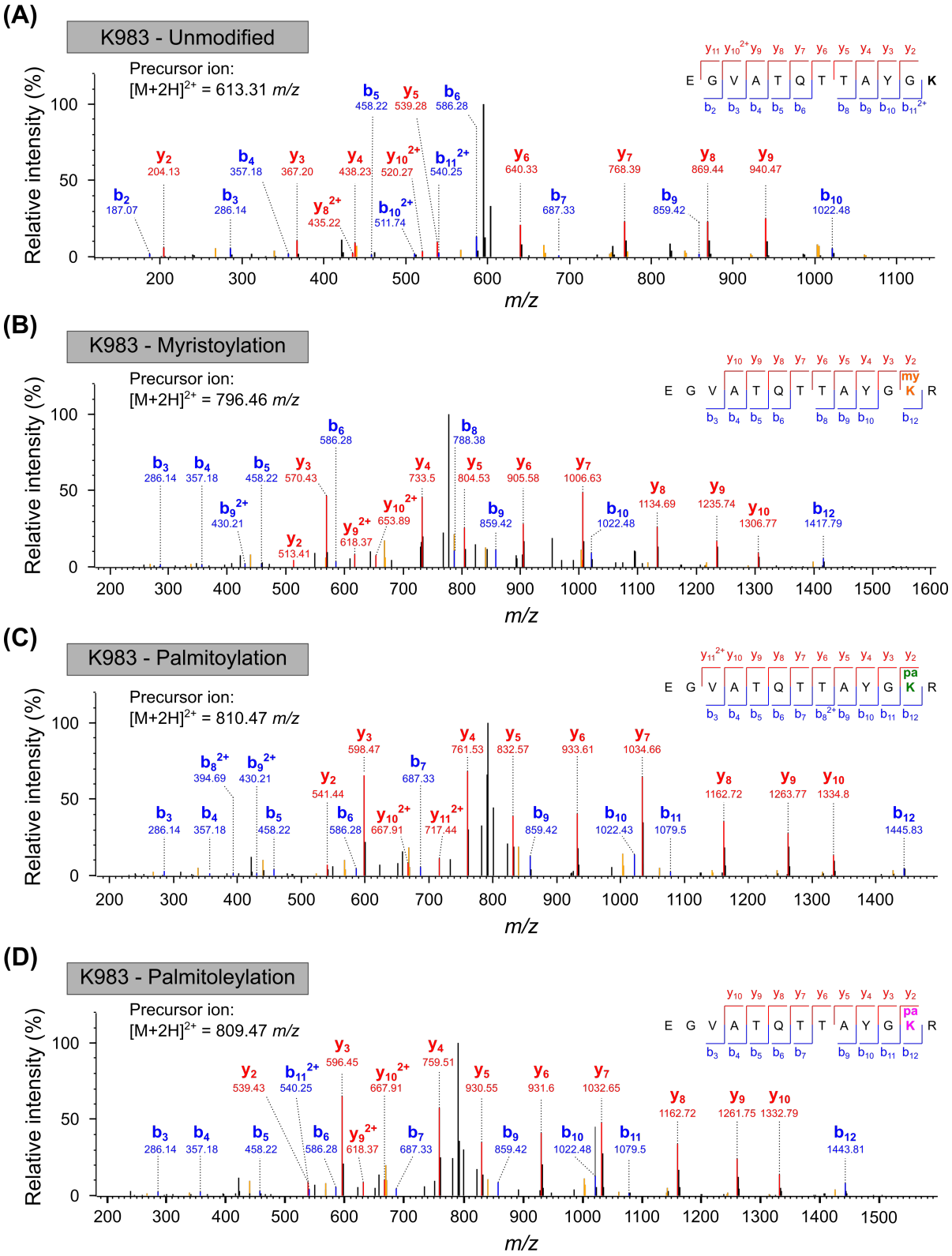

Supplemental Figure S1A: Annotated MS/MS spectrum showing the three distinct PTMs detected at residue K983 in the CyaA toxin: (A) unmodified residue, (B) myristoylated K983, (C) palmitoylated K983, and (D) palmitoleylated K983.

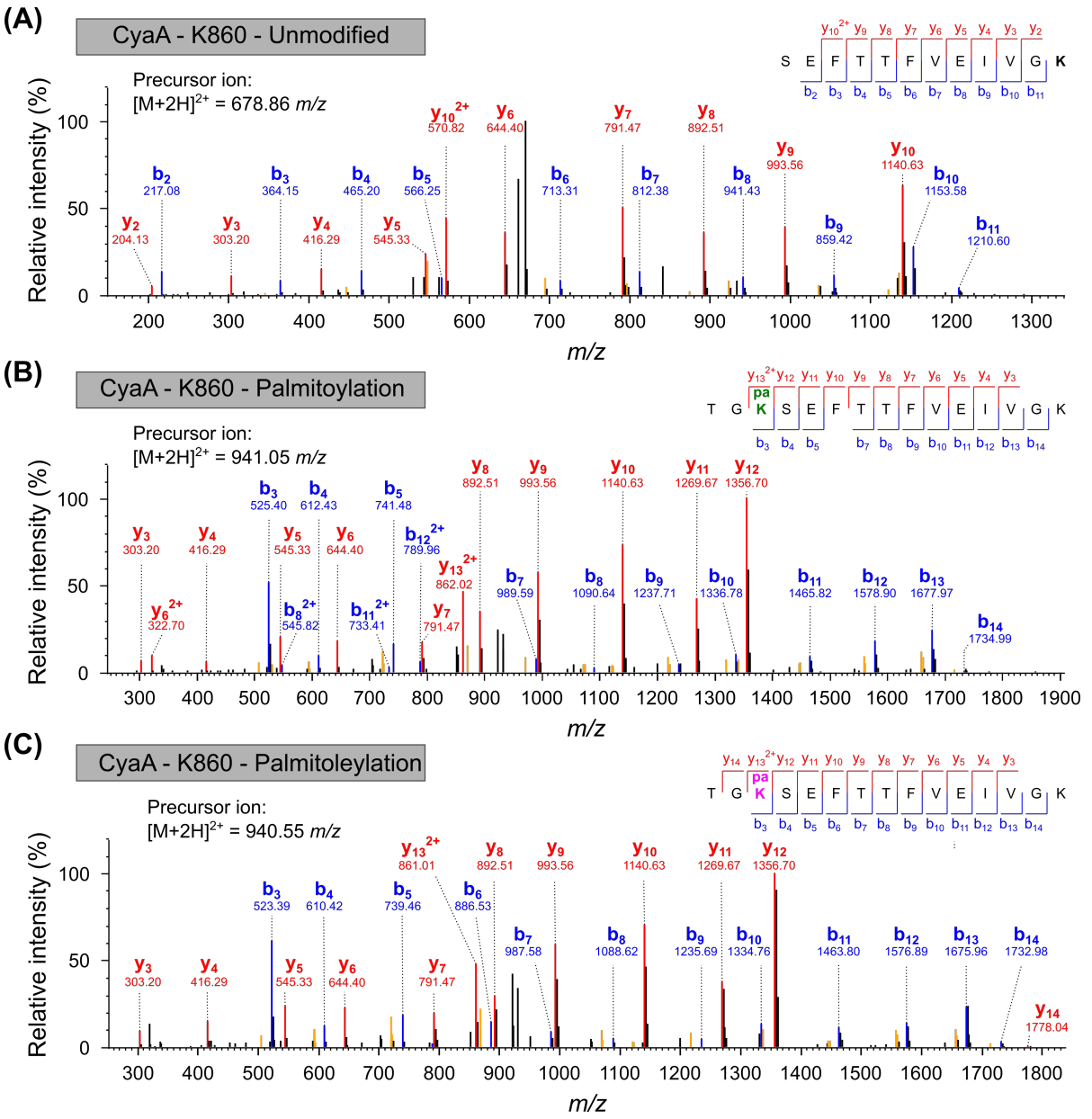

Supplemental Figure S1B: Annotated MS/MS spectrum showing the two PTMs detected at residue K960 in the CyaA toxin: (A) unmodified residue, (B) palmitoylated K860, and (C) palmitoleylated K860.

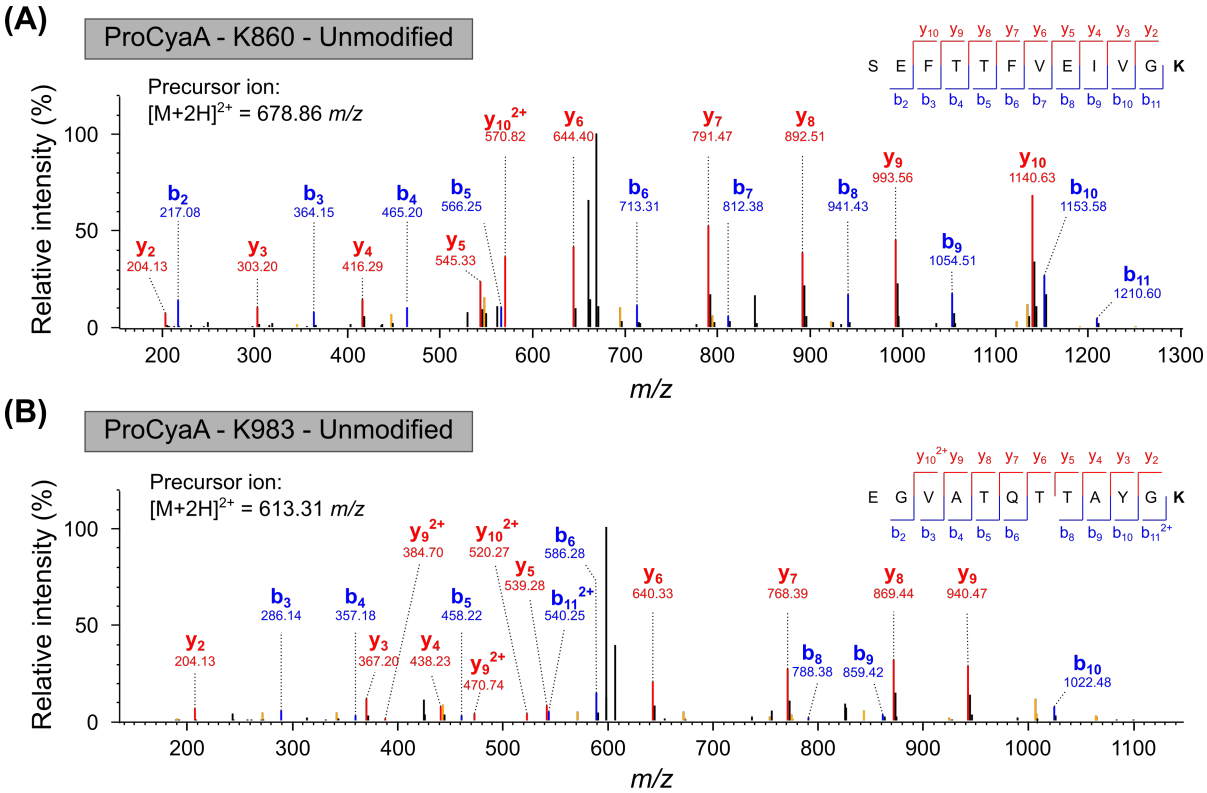

Supplemental Figure S1C: Annotated MS/MS spectrum of the two peptides containing the unmodified K860 (A) and K983 (B) residues in the pro-CyaA toxin.

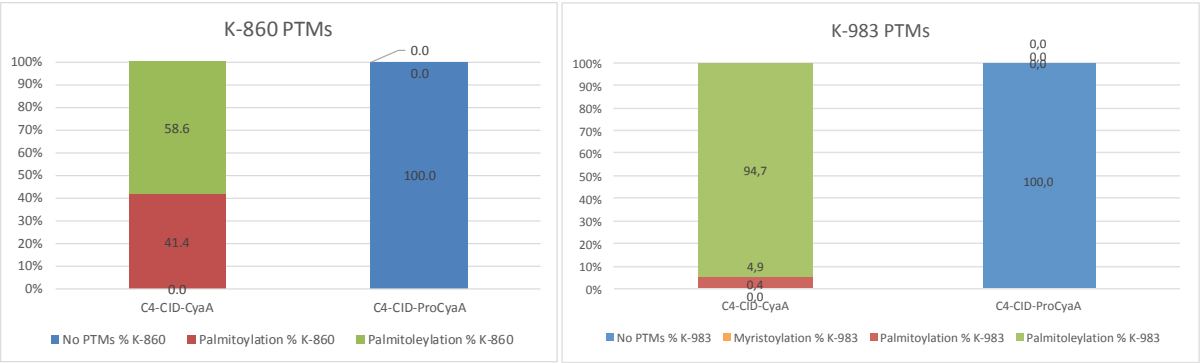

Supplemental Figure S1D: Semi-quantification of K860 and K983 acylation of both CyaA and pro-CyaA monomers from high quality MS/MS spectra. The two lysine residues are always found unmodified in pro-CyaA and acylated in CyaA. We cannot rule-out the possibility that a small fraction of CyaA remains unmodified, but the abundance of such peptides appears too low to be detected by the latest generation of LC-MS Orbitrap instrument used in this study. Absence of PTM on the lysine residue is in blue, palmitoylation in red, palmitoyleylation in green and myristoylation in yellow. Maybe you can briefly explain how was done the quantification with the CID data set.

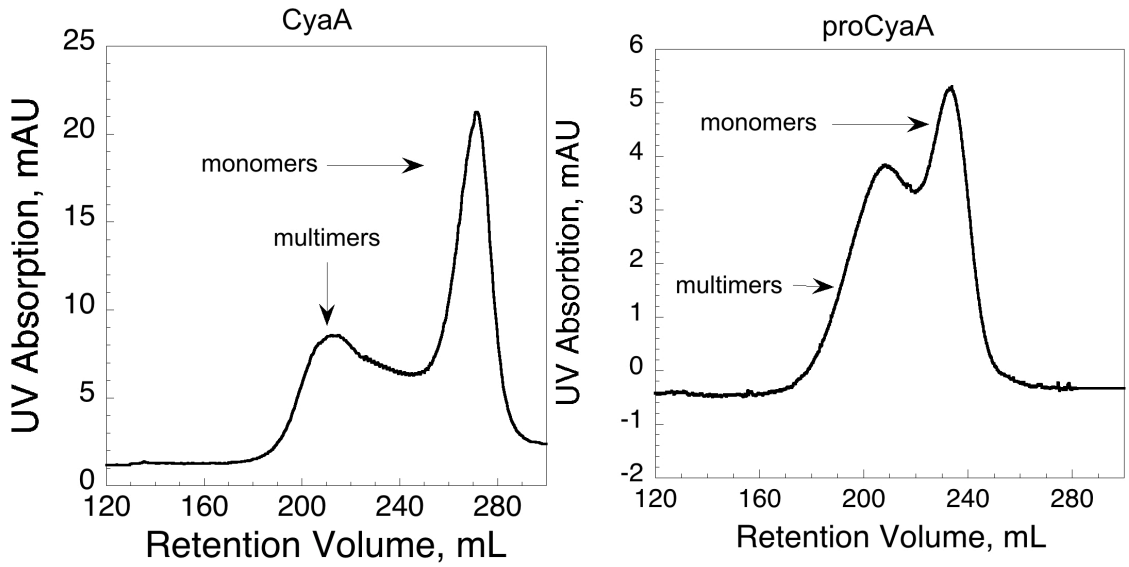

Supplemental Figure S2: Refolding of CyaA and pro-CyaA into a monomeric toxin. The protein is refolded by Size Exclusion Chromatography, using a HiLoad 16/600 Superdex 200 pg column (GE Healthcare), as described in Karst *et al.,* 2014. Briefly, the Superdex 200 pg was equilibrated with buffer A (20 mM Hepes, 150 mM NaCl, pH 7.4), complemented with 2 mM $CaCl_2$. The sample consists of 5 mL of CyaA at 5 µM or 5 mL of proCyaA at 2 µM stored in 8 mM urea, 20 mM Hepes, pH 7.4. After elution, monomers and multimers were pooled separately. Proteins were then concentrated and their hydrodynamic radius measured. Proteins were aliquoted and stored at -20°C. Note the difference of elution volume between the two monomeric species, CyaA and pro-CyaA, in agreement with the AUC data (CyaA monomers are more compact than pro-CyaA monomers).

Supplemental Figure S3: Peptide map of full-length CyaA in the presence of urea. A sequence coverage map was determined after 2 min digestion with pepsin. Each blue bar represents a single CyaA peptide. A linear sequence coverage of 85.7% was achieved. The position of the post-translational acylation sites at K860 and K983 are highlighted by gold stars.

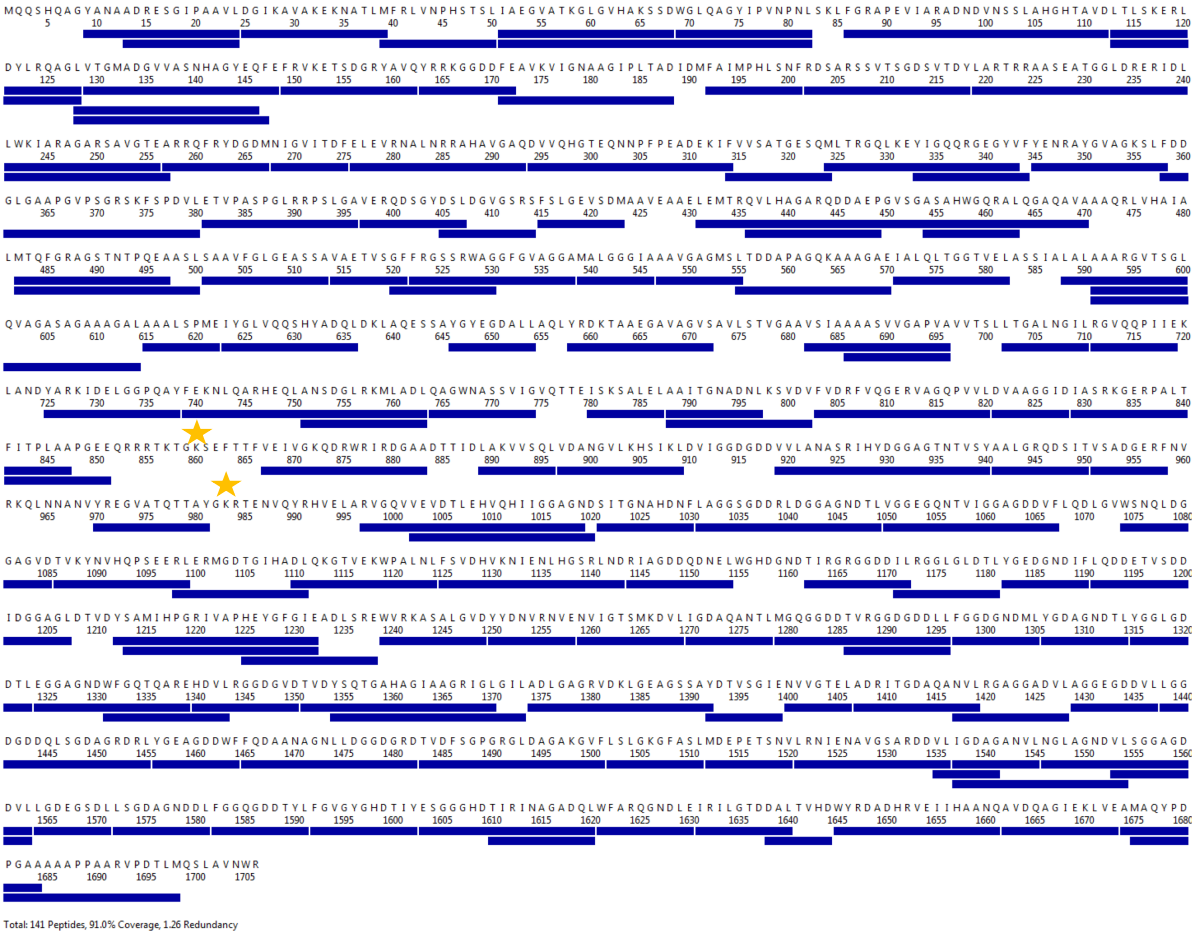

Supplemental Figure S4: Peptide map of native CyaA monomers. A sequence coverage map was determined after 2 min digestion with pepsin. Each blue bar represents a single CyaA peptide. A linear sequence coverage of 91.0% was achieved. The position of the post-translational acylation sites at K860 and K983 are highlighted by gold stars.

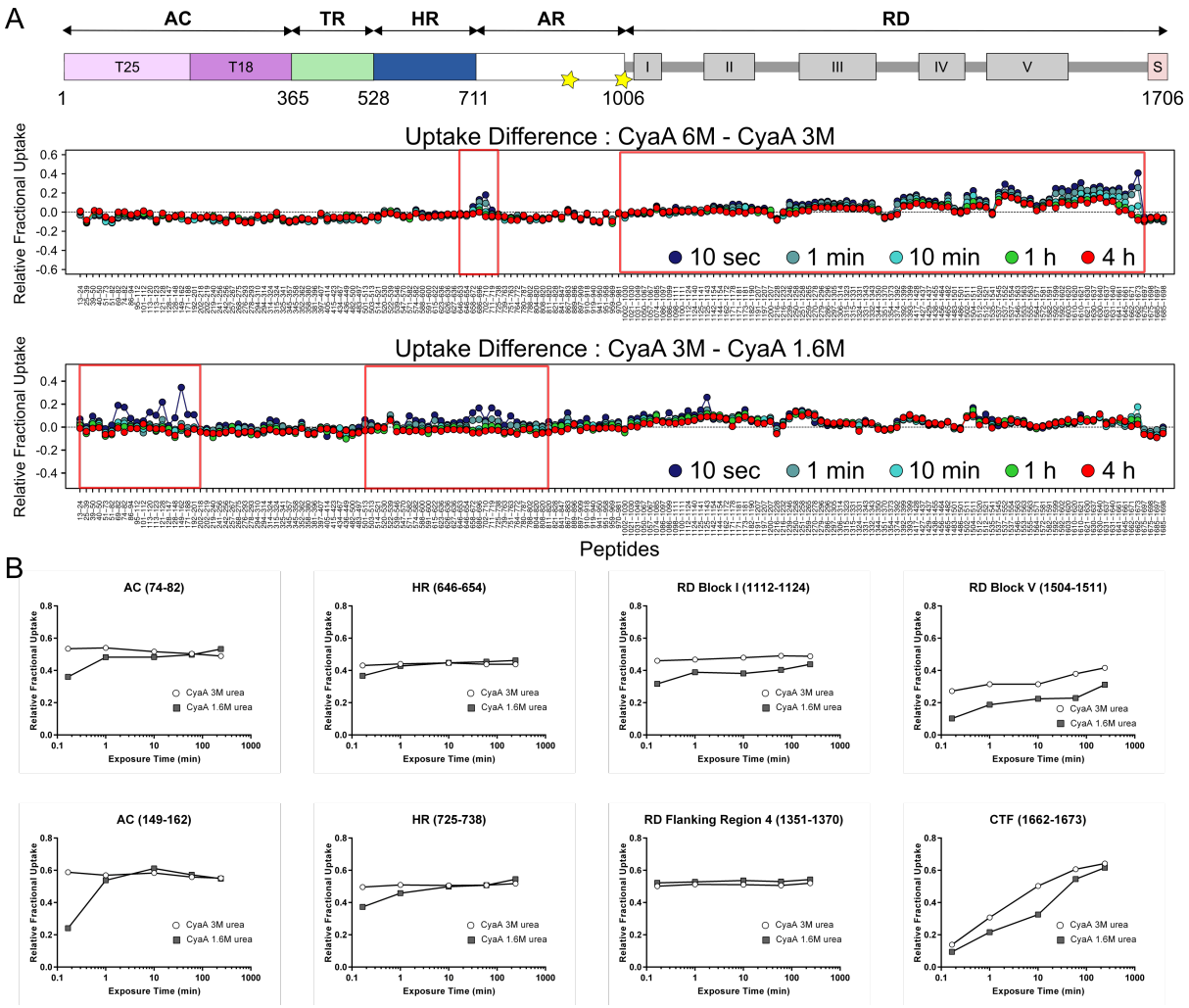

Supplemental Figure S5: Differences in amide hydrogen exchange of CyaA at varying urea concentrations. The structural organization of each domain is displayed in Panel A. Selected peptides displaying unique HDX-MS behaviors in each of the AC, HR and RD domains are given in Panel B. Buffer: buffer A, complemented with 2 mM CaCl2.

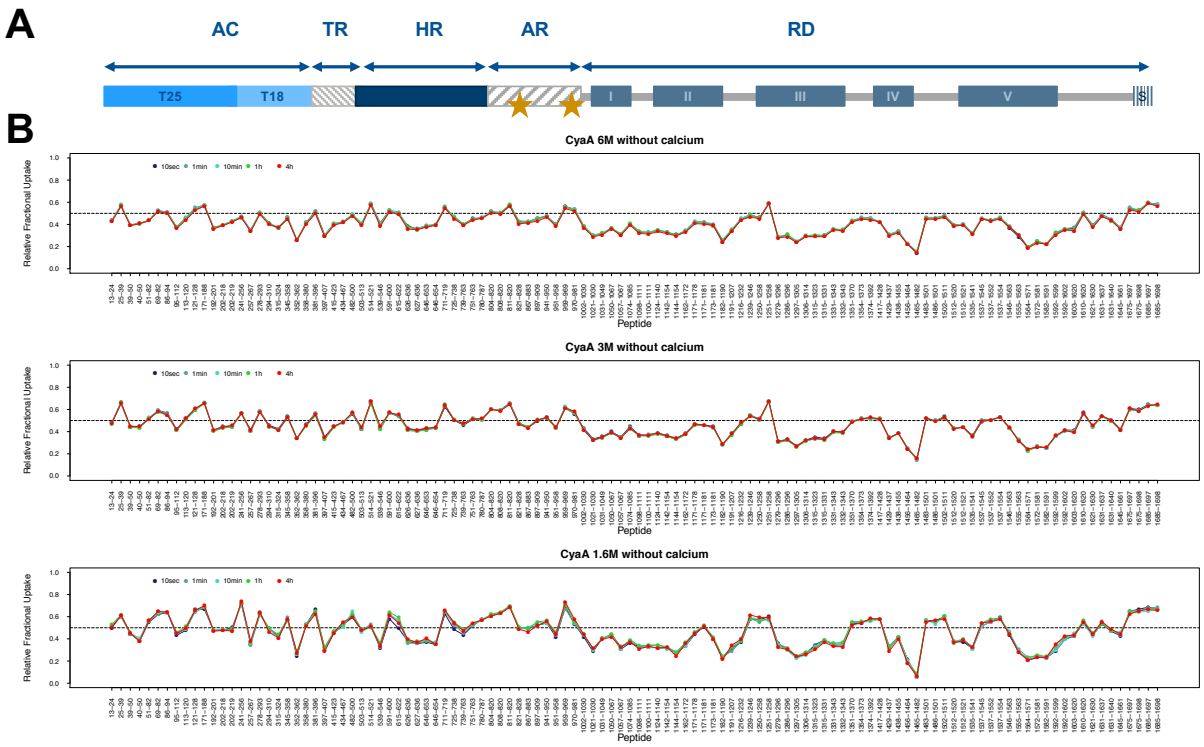

Supplemental Figure S6: Differences in amide hydrogen exchange of CyaA at varying urea concentrations in the absence of calcium. The structural organisation of each domain is displayed in Panel A. The HDX-MS behaviour of CyaA in various concentrations of urea is displayed in Panel B. It is evident that in the absence of calcium, no dynamic HDX-MS behaviour is observed in any region of the protein, regardless of the urea concentration. Buffer: buffer A (20 mM Hepes, 150 mM NaCl, pH 7.4), complemented with 2 mM EDTA.

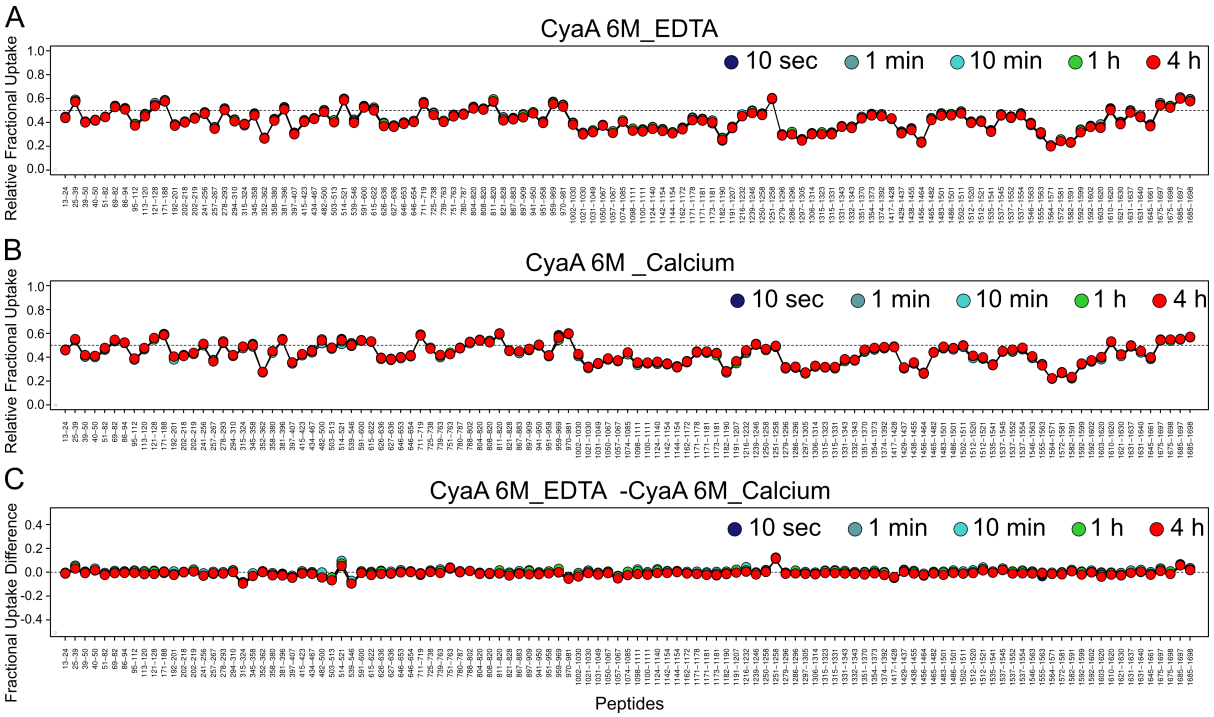

Supplemental Figure S7: Effect of Calcium on the deuterium uptake behavior of CyaA in 6M urea. (A,B) Deuterium uptake profiles of CyaA monitored for each peptide in the presence of 2 mM EDTA (A) or 2 mM Calcium (B). (C) Fractional uptake differential plot generated by subtracting the uptake measured for each peptide and at each time point in the absence (EDTA) and presence of Calcium. A positive difference value indicates a calcium-induced reduction of solvent accessibility.

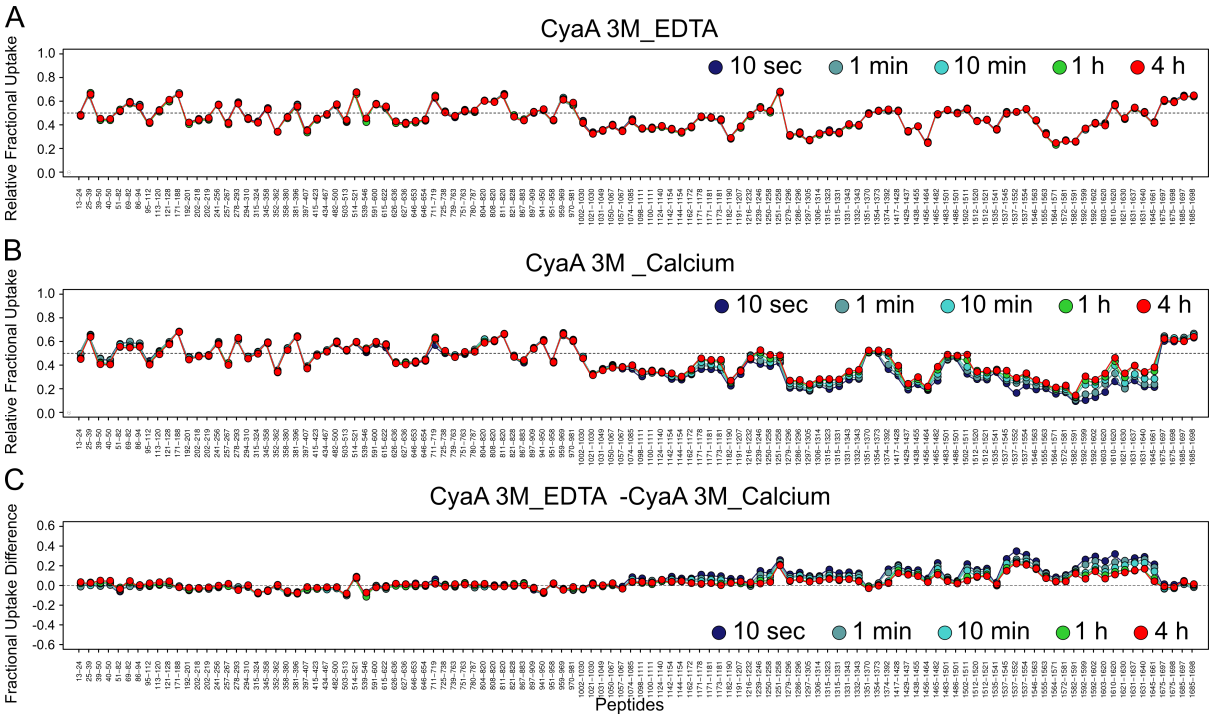

Supplemental Figure S8: Effect of Calcium on the deuterium uptake behavior of CyaA in 3M urea. (A,B) Deuterium uptake profiles of CyaA monitored for each peptide in the presence of 2 mM EDTA (A) or 2 mM Calcium (B). (C) Fractional uptake differential plot generated by subtracting the uptake measured for each peptide and at each time point in the absence (EDTA) and presence of Calcium. A positive difference value indicates a calcium-induced reduction of solvent accessibility.

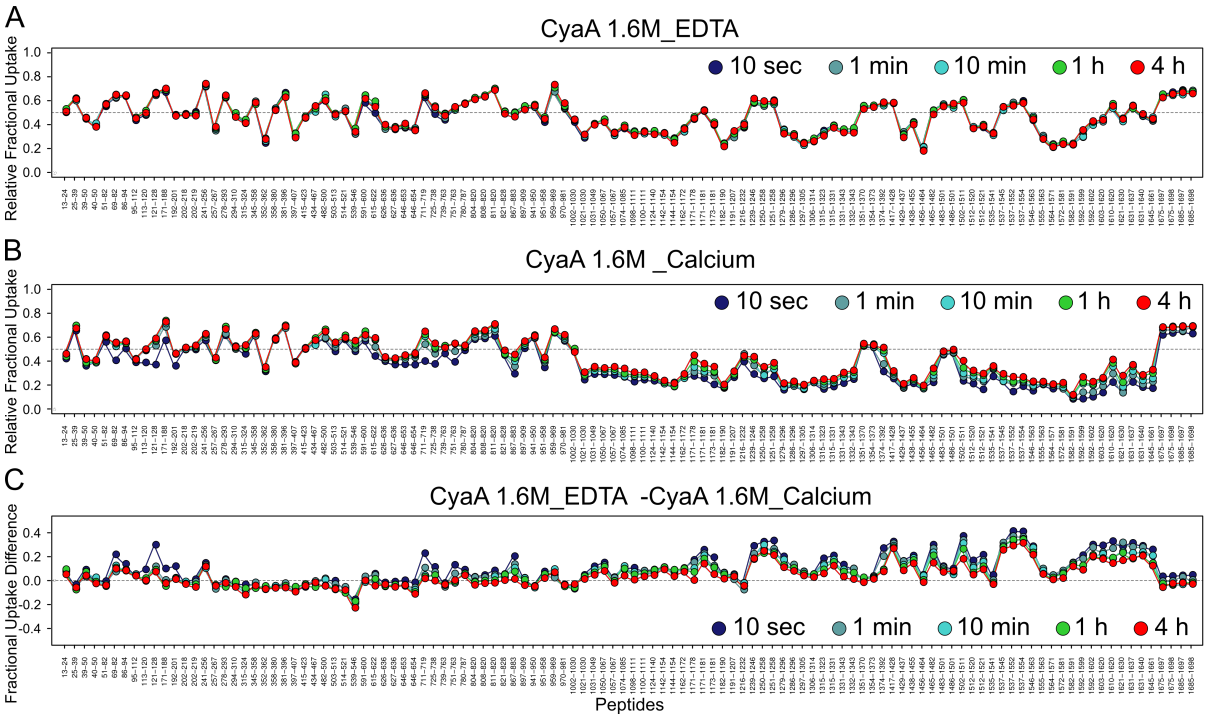

Supplemental Figure S9: Effect of Calcium on the deuterium uptake behavior of CyaA in 1.6M urea. (A,B) Deuterium uptake profiles of CyaA monitored for each peptide in the presence of 2 mM EDTA (A) or 2 mM Calcium (B). (C) Fractional uptake differential plot generated by subtracting the uptake measured for each peptide and at each time point in the absence (EDTA) and presence of Calcium. A positive difference value indicates a calcium-induced reduction of solvent accessibility.

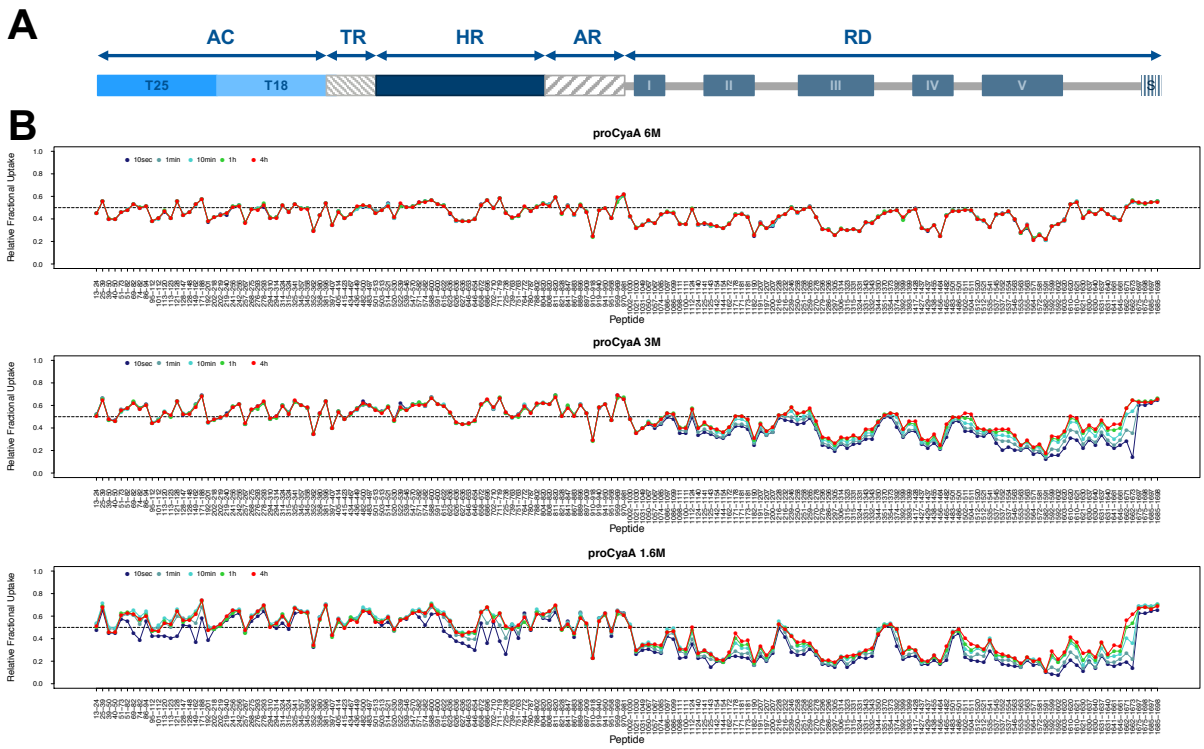

Supplemental Figure S10: Differences in amide hydrogen exchange of pro-CyaA at varying urea concentrations. The structural organisation of each domain is displayed in Panel A. The HDX-MS behaviour of pro-CyaA in various concentrations of urea is displayed in Panel B. At 6 M urea, no dynamic HDX-MS behaviour is observed throughout the protein. At 3 M urea, only the RD region displays dynamic activity. At 1.6 M urea, the AC, HR and RD domains have dynamic HDX-MS events. Buffer: buffer A, complemented with 2 mM CaCl2.

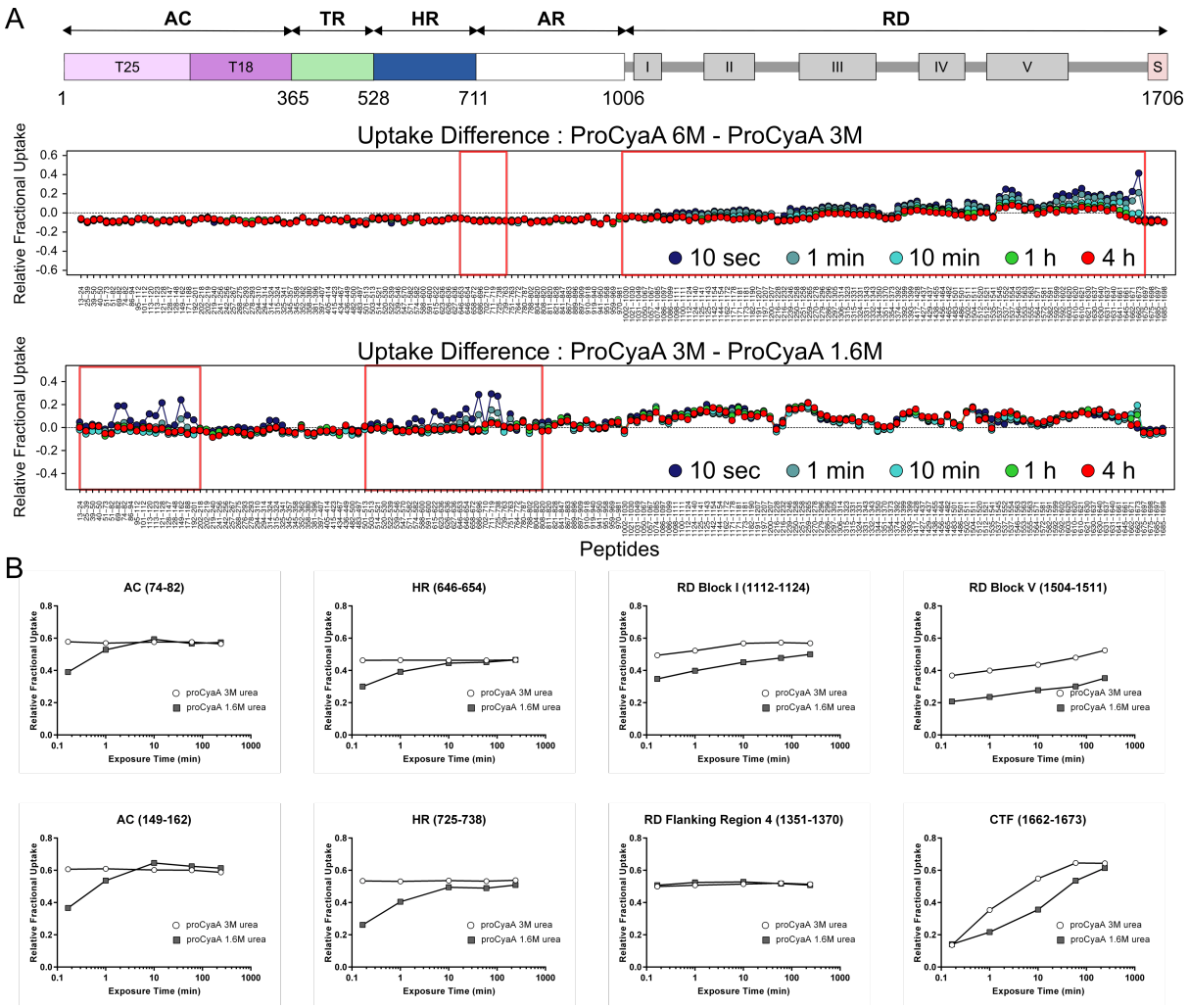

Supplemental Figure S11: Differences in amide hydrogen exchange of pro-CyaA at varying urea concentrations. The structural organization of each domain is displayed in Panel A. Selected peptides displaying unique HDX-MS behaviors in each of the AC, HR and RD domains are given in Panel B. Note that the uptake difference 6 M – 3 M in pro-CyaA shows no fractional uptake difference in HR (see the red box) while in CyaA it does (Supplemental Figure S5A). Buffer: buffer A, complemented with 2 mM CaCl2.

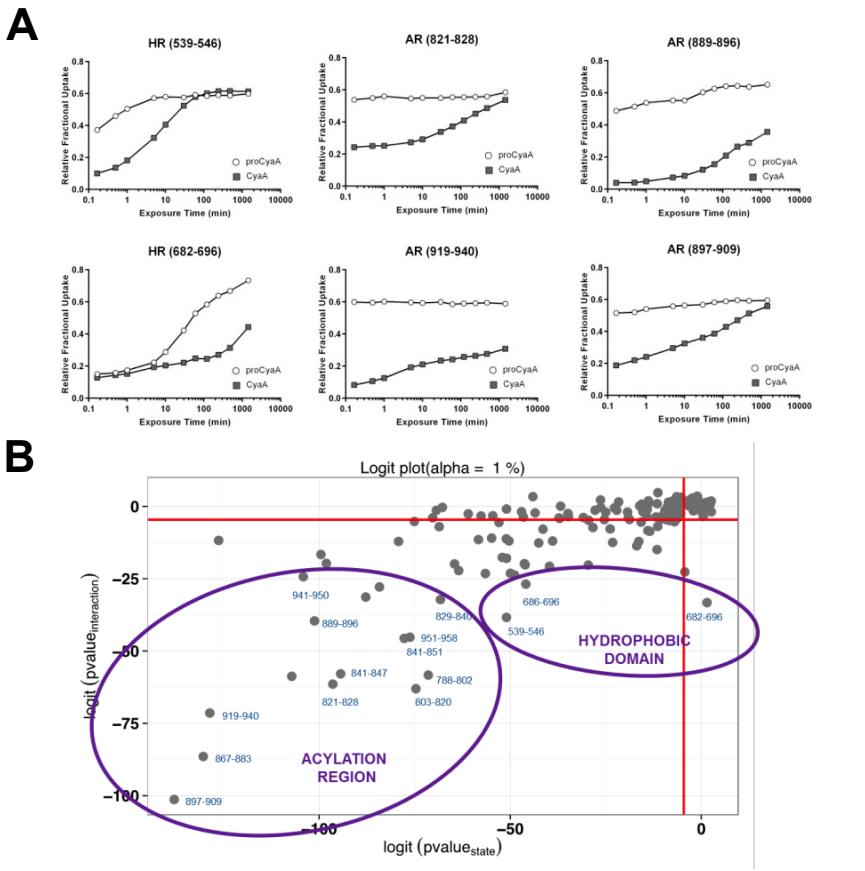

Supplemental Figure S12: Differences in HDX-MS behaviour between monomeric pro-CyaA and CyaA. Panel A displays peptides located in both the HR and AR domains and which give the greatest differences in HDX-MS activity between the two proteins. Panel B displays a Logit representation of the data. Peptides within the AR and HR domains cluster together and independently of each other, demonstrating significant and unique HDX-MS behaviours between the two.

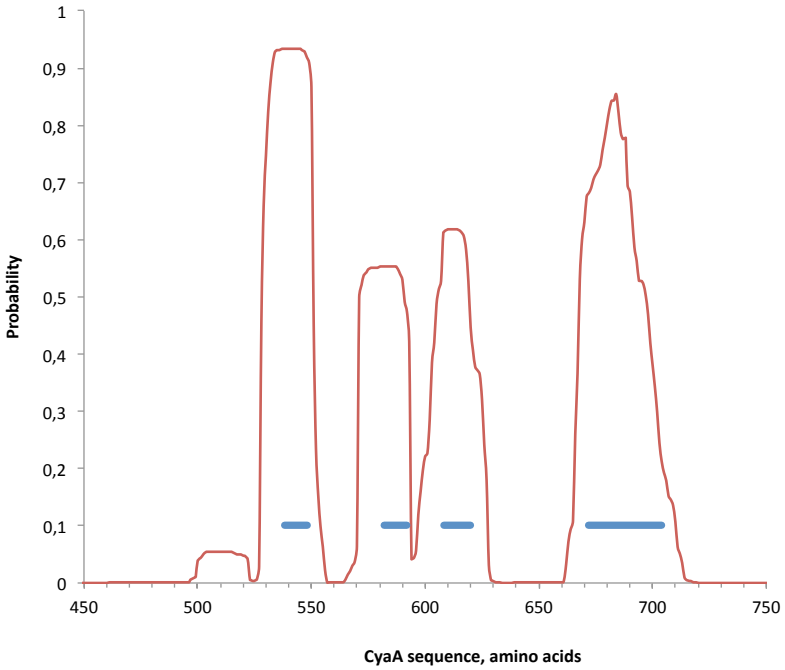

Supplemental Figure S13: Hydrophobicity of the primary structure of the CyaA toxin computed using TMHMM (red trace) and PHD transmembrane helix (blue) prediction servers (1, 2). Major changes observed by HDX-MS between the hydrophobic regions of CyaA and pro-CyaA monomers (peptides 539-546, 571-582, 615-622, 682-696, 686-696 and 702-710 see Figures 5 and 6 for details) are located within the predicted hydrophobic regions.
TMHMM is available here:
http://www.cbs.dtu.dk/services/TMHMM/
PHD transmembrane helix prediction is available here:
https://npsa-prabi.ibcp.fr/cgi-bin/npsa_automat.pl?page=/NPSA/npsa_htm.html

	Proteins	Assay conditions	Hemolysis (%)	Bound Activity (% total)	Internalized Activity (% total)
1	CyaA in urea	$CaCl_2$	87 ± 8	2.14	1.55
		EDTA	< 2.0	0.02	< 0.01
2	Monomeric CyaA	$CaCl_2$	100 ± 6	2.70	0.85
		EDTA	< 2.0	0.34	< 0.01
3	Multimeric CyaA	$CaCl_2$	14 ± 9	2.93	< 0.01
		EDTA	< 2.0	0.39	< 0.01
4	Pro-CyaA in urea	$CaCl_2$	< 2.0	0.03	< 0.01
		EDTA	< 2.0	< 0.01	< 0.01

Supplemental Table S1: Hemolytic and cytotoxic activities of the different CyaA species. Toxin binding and translocation into sheep erythrocytes were assayed essentially as described in Karimova *et al.,* 1998 (3). Adenylate cyclase activity was measured as described in Ladant *et al.*, 1988 (4): 1 unit of adenylate cyclase activity corresponds to 1 µmol of cAMP formed in min at 30°C and pH 8.0. The different CyaA preparations were diluted directly to final concentrations of 5.6-11 nM (1-2 µg/mL) into suspensions of sheep erythrocytes (5×10^8/mL) in buffer A (20 mM Hepes-Na, pH 7.5, 150 mM NaCl) supplemented with either 2 mM $CaCl_2$ or 1 mM EDTA and incubated at 30°C for 20 min. An aliquot was removed to determine the total adenylate cyclase activity added to each sample. The cell suspensions were chilled on ice and centrifuged at 4°C, and the pelleted cells were resuspended in buffer A and separated into two batches. One batch was centrifuged again and the pelleted cells were lysed with 0.1% Tween 20. The enzymatic activity measured in this extract corresponds to that of the toxin bound to the cells and was expressed as a percentage of total activity added to the cells. To the second batch, 20 µg of TPCK (L-1-(tosylamino)-2-phenylethyl chloromethyl ketone)-treated trypsin (Sigma) were added and the mixture was incubated for 10 min at room temperature to digest the adenylate cyclase that remained at the external surface of the erythrocytes. After addition of soybean trypsin inhibitor (5- fold excess), the erythrocytes were washed again with buffer A and then lysed with 0.1% Tween 20. The adenylate cyclase activity protected from trypsin digestion, corresponding to the internalized AC activity, was then measured and expressed as a percentage of total activity added. Activities are expressed as percentages of total CyaA activity added to the erythrocytes suspension (taken as 100%) and represent the average values (with standard deviations below 20 %) from at least two independent measurements. Results are in good agreement with prior studies that showed that about 2-3 % of total CyaA can bind to erythrocytes while 0.5-1.5 % can be internalized in the presence of calcium (3, 5). The hemolytic activity was measured after overnight incubation at 37°C with 60 nM of indicated proteins by quantifying the amount of hemoglobin released at 540 nm (and of intracellular content released at 405 nm). Complete lysis (corresponding to 100% lysis) was obtained by the addition of 0.1% Triton.

Protein species	CyaA monomers	Pro-CyaA monomers
Sedimentation coefficient, S	7.4 ± 0.1	7.1 ± 0.1
R_H, nm	5.5 ± 0.1	5.8 ± 0.1
Solvent density, $g.mL^{-1}$	1.006	1.006
Solvent viscosity, $g.cm^{-1}.s^{-1}$	0.013	0.013
Molecular mass, kDa	177	177
Partial specific volume, $mL.g^{-1}$	0.725	0.725

Supplemental Table S2: Hydrodynamic parameters of CyaA and pro-CyaA monomers measured by AUC. AUC velocity analysis was performed at 20°C as described in Material and Methods. Buffer: 20 mM Hepes, 150 mM NaCl, 2 mM $CaCl_2$, pH 7.4. Experimental details are provided in the material and methods section.

Units used for AUC experiments:

Sedimentation coefficient, S, Svedberg, 10^{-13} sec

Hydrodynamic radius of the protein, R_H, nm

Solvent density, ρ, g/mL

Solvent viscosity, η, poise ($g.cm^{-1}.s^{-1}$)

Molecular Mass, M, kDa

Partial specific volume, $\bar{v}$, mL/g

Supplemental references

1. Combet, C., Blanchet, C., Geourjon, C., and Deleage, G. (2000) NPS@: network protein sequence analysis. *Trends Biochem Sci* **25**, 147-150
2. Krogh, A., Larsson, B., von Heijne, G., and Sonnhammer, E. L. (2001) Predicting transmembrane protein topology with a hidden Markov model: application to complete genomes. *Journal of molecular biology* **305**, 567-580
3. Karimova, G., Fayolle, C., Gmira, S., Ullmann, A., Leclerc, C., and Ladant, D. (1998) Charge-dependent translocation of Bordetella pertussis adenylate cyclase toxin into eukaryotic cells: implication for the in vivo delivery of CD8(+) T cell epitopes into antigen-presenting cells. *Proc Natl Acad Sci U S A* **95**, 12532-12537
4. Ladant, D. (1988) Interaction of Bordetella pertussis adenylate cyclase with calmodulin. Identification of two separated calmodulin-binding domains. *J Biol Chem* **263**, 2612-2618
5. Gmira, S., Karimova, G., and Ladant, D. (2001) Characterization of recombinant Bordetella pertussis adenylate cyclase toxins carrying passenger proteins. *Res Microbiol* **152**, 889-900